Journal of Advanced Scientific Research
Available online through https://sciensage.info
ISSN
0976-9595
Research Article

INVESTIGATIONS ON THE GROWTH AND CHARACTERIZATION OF MAGNESIUM SULFATE DOPED L-LEUCINIUM OXALATE CRYSTALS

Gershom Jebaraj P.*[1], SivashankarV.[2]
[1]*Reg. No.: 18231282131041, Crystal Research Centre, Department of Physics, St. Xavier's College (Autonomous), Palayamkottai, Tamilnadu, India*
[2]*Department of Physics, St. Xavier's College (Autonomous), Palayamkottai, Tamilnadu, India*
(Affiliated to Manonmaniam Sundaranar University, Abishekapatti, Tirunelveli, Tamilnadu, India)
**Corresponding author: gershomjeba@gmail.com*
Received: 13-07-2022; Accepted: 12-09-2022; Published: 30-09-2022
 https://doi.org/10.55218/JASR.202200000

ABSTRACT
Magnesium Sulfate-doped L-Leucinium oxalate (MSLO) single crystal was grown using slow evaporation method. Structure of the crystal was determined by single-crystal X-Ray Diffraction (XRD). Lattice parameters of MSLO crystal were determined. Optical transmittance study was done to find various linear optical parameters like band gap, reflectance, refractive index, absorption coefficient, extinction coefficient, optical conductivity. Vickers Micro hardness study was carried out to find mechanical properties such as hardness, work hardening coefficient, brittleness index and fracture toughness of the grown MSLO crystal. Kurtz-Perry powder technique with Nd: YAG laser was applied to study the second harmonic generation (SHG) competency. By using Z-scan technique, third-order NLO efficiency of MSLO crystal was calculated. LDT study was also done for MSLO crystal. It is observed that magnesium sulfate-doped L-leucinium oxalate (MSLO) crystal has the superior properties compared to that of undoped L-leucinium oxalate crystal. EDS studies were conducted for MSLO crystal to check the elements present in the crystal.

Keywords: Growth, XRD, optical conductivity, impedance, Microhardness, SHG, LDT.

1. INTRODUCTION
Non Linear Optical (NLO) crystals are being considered largely due to their widespread applications in optical communication, optical computing, optical information processing, laser technology and photonics [1, 2]. Non-centrosymmetric organic compounds have second-order nonlinear optical features and they are superior to inorganics [3-5]. It is known that, amino acid complexes are found to be important NLO materials for the development of devices. Many amino acids reveal nonlinear optical properties, due to the presence of donor NH_3^+ and acceptor COO^- as well as the chance of intermolecular charge transfer [6, 7]. Many number of studies have been described on the characteristics of amino acid complexes and organic, inorganic and semi organic NLO crystalline samples have been grown and studied by differentauthors [8-10].Anbuchezhiyan et al. have grown the crystal of undoped L-leucinium oxalate. It was characterized by XRD, CHN, FTIR, NMR, NLO, optical and hardness studies [11]. Bhaskaran *et al.* have carried out thermal, optical, electrical properties of L-leucinium oxalate crystal [12]. In this work, L-leucinium oxalateis considered as the base material and doping of an inorganic material like magnesium sulfate was done to alter various properties of the host crystal. The growth, single crystal XRD, optical, SHG, mechanical, impedance and laser damage threshold (LDT) properties of magnesium sulfate-doped L-leucinium oxalate (MSLO) crystals are explained in this communication.

2. MATERIAL AND METHODS
The AR grade chemicals such as L-leucine, oxalic acid and magnesium sulfate with high purity were purchased. Slow evaporation crystal growth method has variety of benefits like low cost, easy growing, controlling the rate of evaporation and re-crystallization to improve the quality of crystal and

hence in this work, this method was followed to grow magnesium sulfate doped L-leucinium oxalate (MSLO) crystal.

L-leucine and oxalic acid in 1:1 molar ratio and 1 mole % of magnesium sulfate were taken and dissolved in double distilled water. Care was taken to consider the solution was a supersaturated solution. Solution was stirred using magnetic stirrer attached with hot plate for about 4 hours. Then the solution was filtered using good quality Whatmann filter papers. The filtered solution was taken in a beaker which is closed by a holed polythene paper. The solution was allowed for slow evaporation. The flow diagram for crystal growth process is presented in fig. 1.

Initially, seed crystals were grown. They were further purified byre-crystallization process [13]. By placing good quality seed crystals in supersaturated solution, single crystal of MSLO crystals were grown after the growth period of 28 days. Schematic Diagram of the reaction mechanism is given in fig. 2. The grown MSLO crystal is depicted in fig. 3. It is observed that the grown MSLO crystal is colourless and transparent. The size of the crystal is 23 × 5 × 5 mm^3.

Fig. 1: Flow diagram for crystal growth process

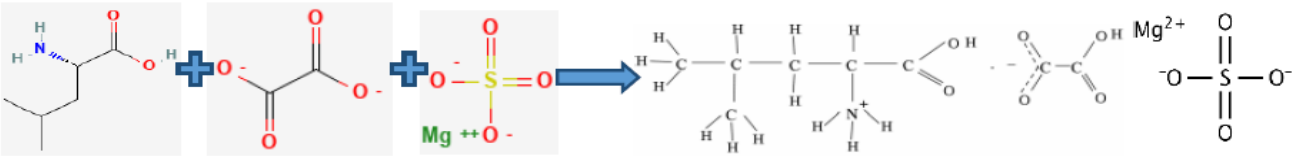

Fig. 2: Reaction Mechanism

Fig. 3: Magnesium Sulfate Doped L-Leucinium Oxalate Crystal

3. RESULTS AND DISCUSSION

3.1. Single crystal X-ray diffraction studies

X-Ray Diffraction (XRD) is the principle to find crystal structure of a crystalline material because it acts like a three-dimensional grating. Single crystal XRD data were measured on a Bruker 4 SMART KAPPA APEX IICCD single-crystal X-ray diffractometer using graphite monochromatized MoK_α radiation (λ= 0.71073 Å). Obtained lattice dimensions of MSLO crystalarea= 5.671(4) Å, b = 9.758(3) Å, c= 9.889(3) Å, and

α=87.54° (3), β=98.83° (2), γ= 101.04° (3)and V= 542.63(4)Å^3. The data reveals that, MSLO crystal crystallizes in triclinic structure with space group P1. It is found that the crystal structure of undoped L-leucinium oxalate [14] is same as compared to that of MSLO crystal but the lattice parameters were slightly changed due to inclusion of magnesium sulfate in the interstitial positions of the lattice of host L-leucinium oxalate crystal. XRD data for MSLO crystal is given in table 1.

Table 1: Single-crystal XRD data for MSLO crystal

1) Identification code	MSLO
2) Empirical formula	$C_6H_{14}NO_2$. C_2HO_4. $MgSO_4$
3) Molecular weight	341.57 g/mol
4) Crystal size (mm^3)	23 × 5 × 5 mm^3
5) Temperature	293(2) K
6) Wavelength	0.71073 Å
7) Crystal system	Triclinic
8) Space group	P1
9) Unit cell parameters (Å)	a = 5.671(4) Å, b = 9.758(3) Å, c = 9.889(3) Å, and α = 87.54°(3), β = 98.83° (2), γ = 101.04° (3)
10) The volume of a unit cell	V = 542.63(4) Å^3.

3.2. UV-Vis spectral characterization

In UV-visible spectroscopy, moving of electrons from lower state to higher energy levels occurs and hence it gives information about the molecule's structure. To record the transmittance spectrum of MSLO crystal, UV-visible spectrophotometer which operates between 190nm and 1100nm was used. The obtained spectrum is depicted in fig.4. The spectrum reveals that the grown MSLO crystal's lower cut-off wavelength is 218 nm.

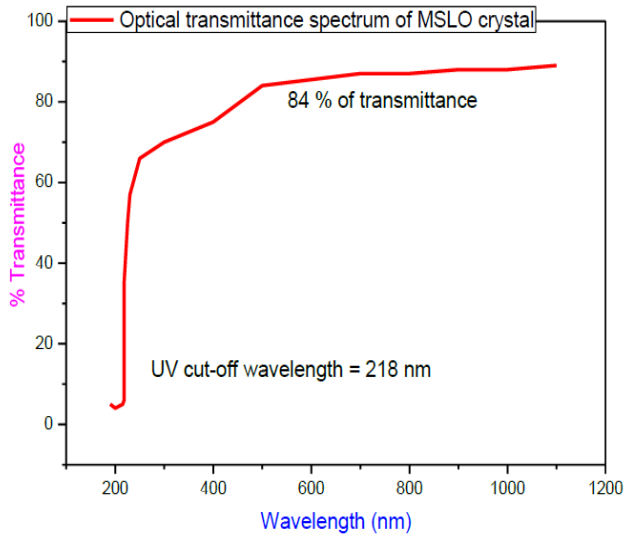

Fig. 4: UV-Vis-NIR transmittance spectrum of MSLO crystal

3.2.1. Band Gap

Optical band gap (E_g) of the sample was determined using the relation Eg= 1240/λ

Where, λ is wavelength of light. The band gap value was determined as 5.69 eV and this value is observed to be high. This indicates that MSLO crystal is an insulating material. The purpose of doing UV-Vis spectral study is to find the transmittance, absorption coefficient, optical band gap, extinction coefficient, optical conductivity, complex dielectric constant and linear refractive index and suitability crystal for nonlinear optical (NLO) applications [15].

3.2.2. Absorption Coefficient

Absorption coefficient (α) is estimated using expression α = [2.303 log (1/T)]t, where T is the transmittance in decimal points and t is the thickness of the crystal. Variation of absorption coefficient with wavelength for MSLO crystal is given in the fig.5.

Tauc's relation is given by

$$\alpha = \frac{A\,(h\nu - Eg)^{1/2}}{h\nu}$$

Where E_g is optical band gap, h is the Planck's constant, ν is frequency and A is a constant [16]. The plot of variation of $(\alpha h\nu)^2$ versus photon energy hν is presented in fig. 6. Optical band gap was evaluated by the extrapolation of the linear part to the X-axis and the

value is found to be 5.70 eV and this value indicates that MSLO crystal is a dielectric material.

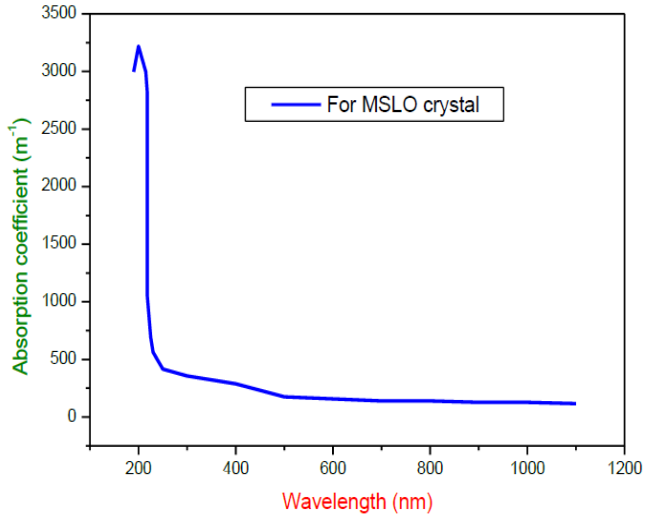

Fig. 5: Plot of absorption coefficient versus wavelength of MSLO crystal

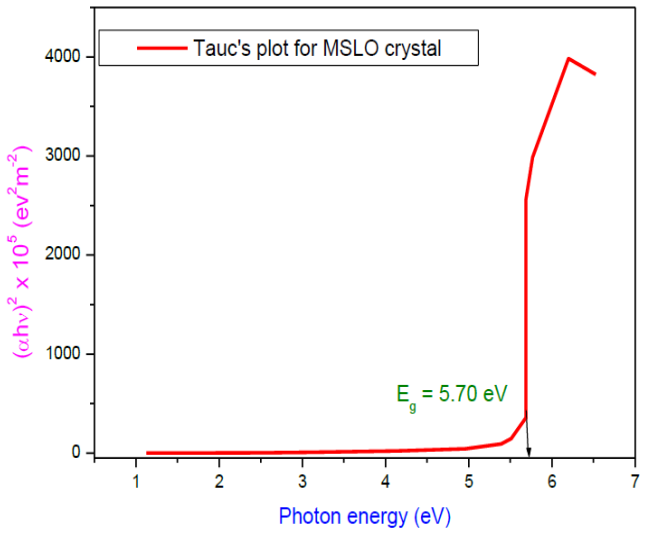

Fig. 6: Tauc's plot for MSLO crystal

3.2.3. Extinction Coefficient

Extinction coefficient is the amount of light energy lost per unit thickness in a given medium due to scattering and absorption. Extinction coefficient of MSLO crystal was calculated using the relation $K = \frac{\alpha\lambda}{4\pi}$ where α is linear absorption coefficient and λ is wavelength of light. Variation of extinction coefficient with wavelength is shown in the fig.7. From the figure, it is observed that, the extinction coefficient is high at fundamental absorption in the UV region. In the wavelength region 500-1000 nm, extinction coefficient increases slightly with increase of wavelength. From the result, it is found that, extinction coefficient of MSLO crystal is very low. It shows the grown Crystal is a good optical material with very low energy loss.

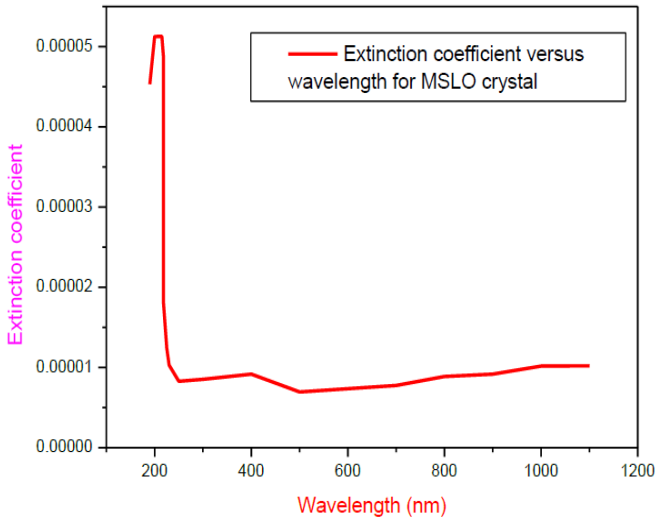

Fig. 7: Plot of extinction coefficient versus wavelength for MSLO crystal

3.2.4. Reflectance

Reflectance is the amount of light energy reflected from the crystal. Expression for reflectance (R) is given below.

$$R = 1 \pm \frac{\sqrt{1 - \exp(-\alpha t) + \exp(\alpha t)}}{1 + \exp(-\alpha t)}$$

Where α is absorption coefficient and t thickness of the sample [17, 18]. The variation of reflectance with wavelength is depicted in the fig.8.Result indicates that the reflectance of the crystal is low.

3.2.5. Linear refractive index

Linear refractive index is the ratio of speed of light in vacuum or free space to the speed of light in the medium and it is determined using the following expression.

$$n = \frac{1 + \sqrt{R}}{1 - \sqrt{R}}$$

Where R is the reflectance in decimal point. Plot of linear refractive index with photon energy for MSLO crystal is presented in fig.9. At high wavelength region, the refractive index is observed to be increasing with increase of photon energy and it is very high near the fundamental absorption region.

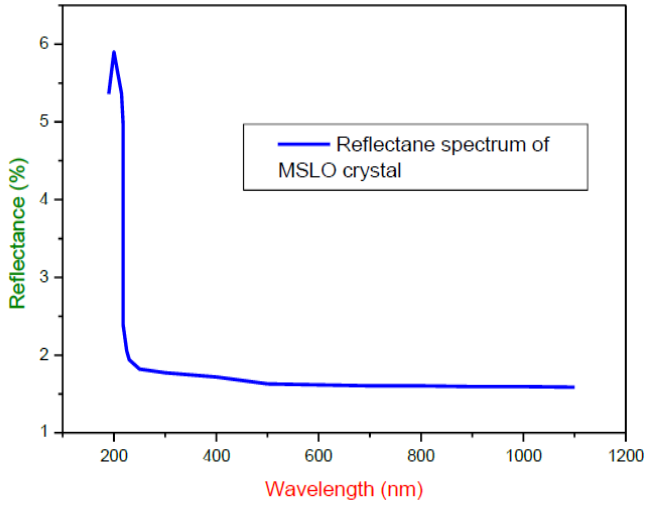

Fig. 8: Reflectance spectrum of MSLO crystal

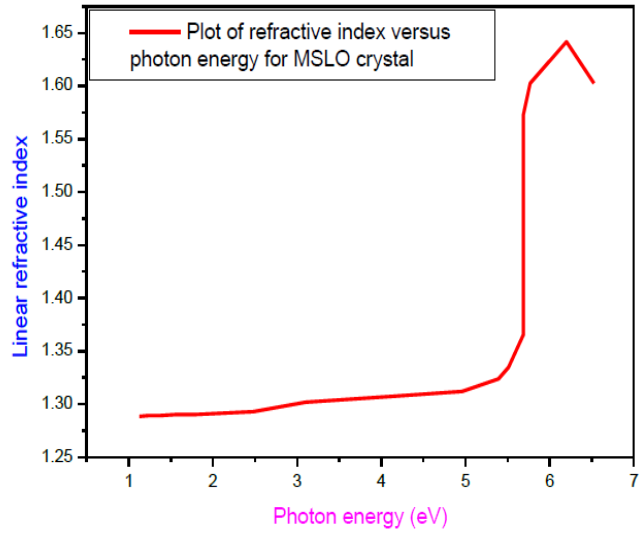

Fig. 9: Variation of refractive index with photon energy for MSLO crystal

3.2.6. Optical conductivity

The optical conductivity of the grown crystal was determined using the following relation.

$$\sigma_{OP} = \varepsilon_0 \, c \, n \, \alpha$$

Where c is the velocity of light in free space, α is the linear absorption coefficient, ε_0 is the permittivity of free space or vacuum and n is the refractive index. As per the relation above, optical conductivity is directly proportional to absorption coefficient and hence a straight line plot is obtained in the fig.10. It is seen that optical conductivity increases as the absorption coefficient increases. The value of optical conductivity of the sample can also be calculated in Gaussian units by using the following relation

$$\sigma_{OP} = \frac{1}{4\pi\varepsilon_0} \, c \, n \, \alpha$$

$$\sigma_{OP} = 9 \times 10^9 \, \varepsilon_0 \, c \, n \, \alpha$$

The above equations have been used [19] to determine the value of optical conductivity. It is shown in the fig.11.

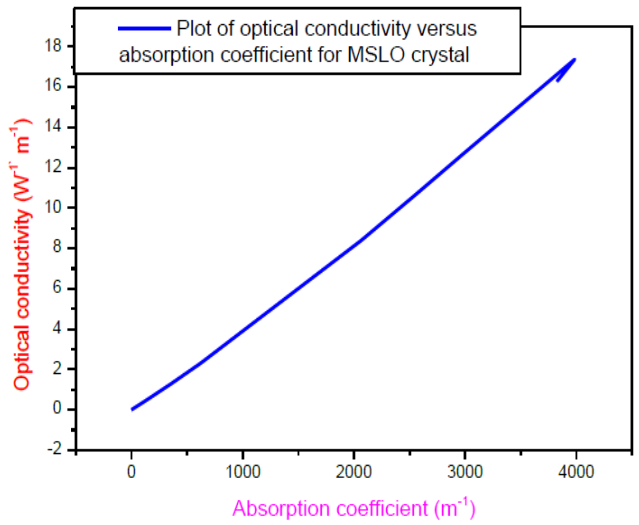

Fig. 10: Plot of optical conductivity (in SI units) versus absorption coefficient for MSLO crystal

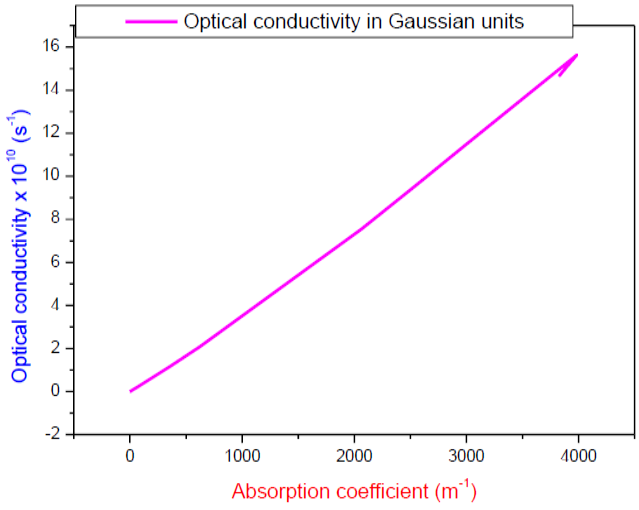

Fig. 11: Plot of optical conductivity (in Gaussian units) versus absorption coefficient for MSLO crystal

3.3. Impedance analysis

Impedance is a parameter opposition to the AC current in a sample. The complex impedance is givenby Z = Z' + jZ" where Z' is the real part of impedance, Z" is the imaginary part of impedance and j is complex parameter. The measurement of impedance provides a

lot of information such as grain boundary resistance, bulk resistance, DC conductivity, electrical relaxation phenomena etc. Impedance measurement for MSLO crystal was carried out using an impedance analyser over the frequency range of 1 Hz-10^6 Hz at 30°C and 50°C. The frequency-dependent real part and imaginary part of impedance for MSLO crystal are given in the figs. 12 and 13.

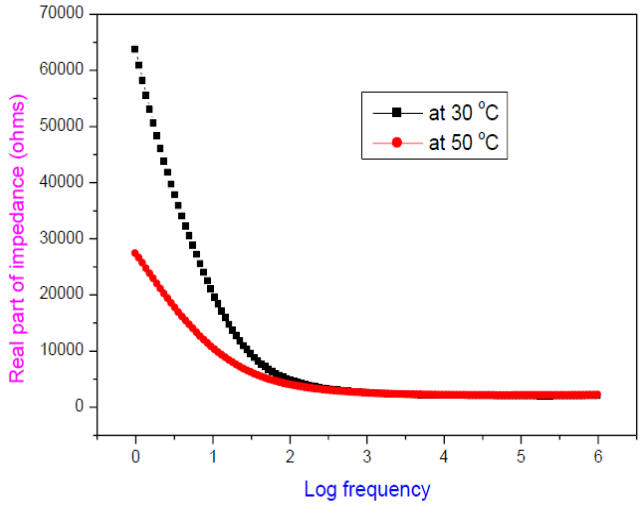

Fig. 12: Real part of impedance variation with frequency at different Temperatures for MSLO crystal

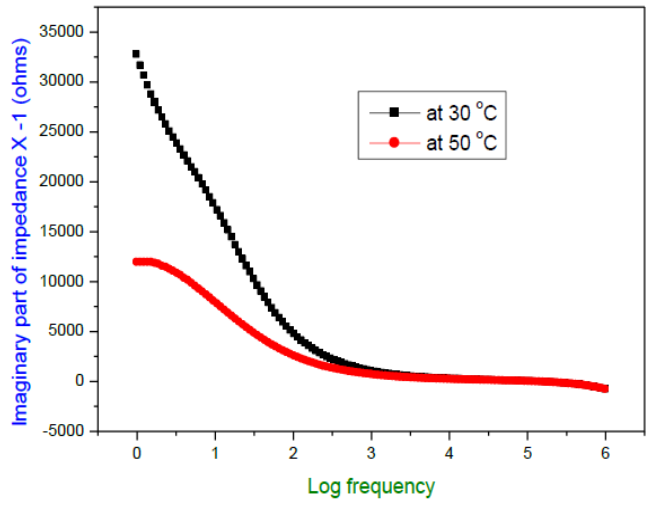

Fig. 13: Imaginary part of impedance variation with frequency at different Temperatures for MSLO crystal

It is noticed from the figures that, as the frequency increases, both the real and imaginary components of impedance decreases and appears to converge at the higher frequency side. This may be due to reduction of space charge polarization. Further, as temperature increases, impedance values increase and this indicates that the sample has negative temperature coefficient.

Nyquist plot of the grown MSLO crystal for different temperatures is shown in fig. 14. The result reveals the electrical characteristics of MSLO crystal are mostly caused by grain boundary and bulk effects [20, 21].

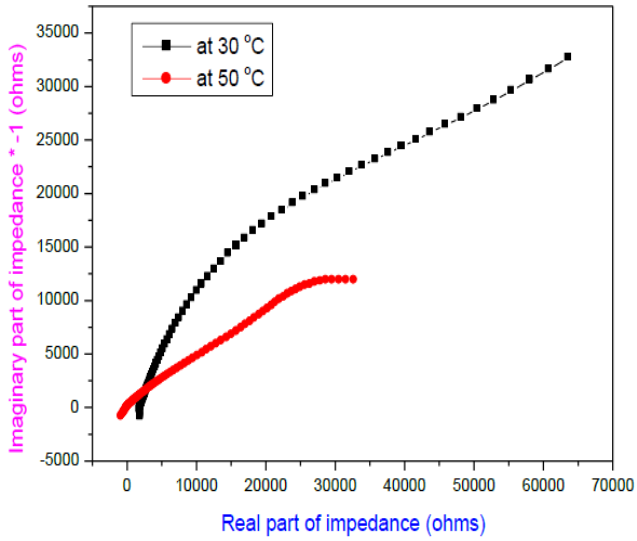

Fig. 14: Nyquist plot of the grown MSLO crystal

3.4. Vickers Microhardness study

Microhardness measurement was carried out using a Vickers Microhardness indenter. Vickers hardness test comes under static indentation test method and this method is used to study the Microhardness of the grown crystals. Information about the strength and deformation characteristics of material shall be obtained from this. Static indentation test is the simplest test, in which, specific geometry is pressed into the surface of specimen with known load. Ball or diamond cone or diamond pyramid intended shall be used. After removal of indenter, a permanent impression will be retained in the specimen. Hardness of the sample shall be calculated from the depth of indentation produced by measuring the cross sectional area or the depth of the indentation. The Vickers hardness number (H_v) or Diamond Pyramid Number (DPN) is estimated using the relation

$$Hv = (1.8554\,P)/d^2$$

Where P is the applied load and d is the average diagonal length of the indented impression and 1.8544 is a constant of a geometrical factor for the diamond pyramid indenter [22]. The variations of average diagonal indentation length (d) with load (P) for the

samples are shown in fig. 15 and it is seen that the values of d are increasing as the applied load increases and value of d of MSLO crystal is observed to be less compared to that of undoped L-leucinium oxalate crystal.

Fig. 16 shows the plots of hardness with applied load for both samples. Hardness is observed to be more for MSLO crystal compared to that of undoped L-leucinium oxalate crystal. Observed high hardness value for MSLO crystal is due to presence of magnesium sulfate in the form of ions in the lattice of L-leucinium oxalate crystal.

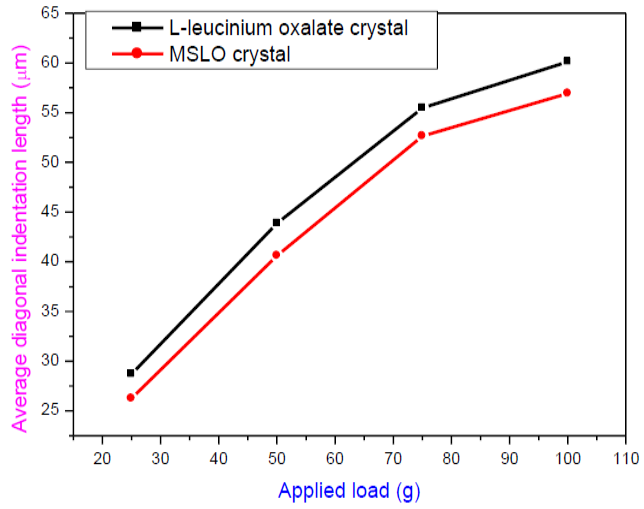

Fig. 15: Plots of average diagonal indentation length versus applied load for undoped and magnesium sulfate-doped L-leucinium oxalate (MSLO) crystal

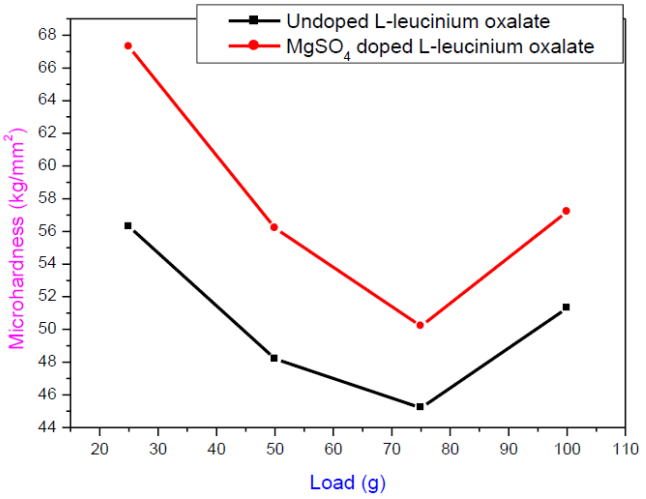

Fig. 16: Plots of Microhardness versus applied load for undoped and Magnesium sulfate-doped L-leucinium oxalate (MSLO) crystal

3.4.1. Work hardening coefficient

Meyer gave a relationship between hardness and work hardening capacity of a material. It is given by $P = (a \times d^n)$ where a and n are constants for a given material. The value of n can be considered as a parameter representing the capacity for work hardening or Meyer's index and it may be determined experimentally by performing the test at various loads. The above relation can be written as log P = log(a) + n log(d) and the slope of the line plotted between log(d) and log(P) gives the value of n. The plots of between log (d) and log (P) for undoped and magnesium sulfate-doped L-leucinium oxalate (MSLO) crystals are presented in the figs. 17 and 18. From the figures, the values of work hardening coefficient are found to be 2.236 and 2.517 respectively for undoped and MSLO crystals. As these values are more than 1.6, the grown crystals are confirmed to be soft category of materials [23, 24].

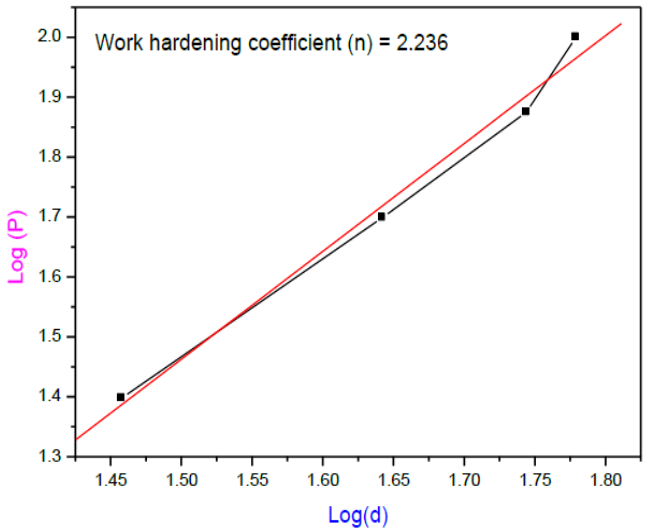

Fig. 17: Plot between log (d) and log (P) for undoped L-leucinium oxalate crystal

3.4.2. Fracture toughness

Fracture toughness (K_c) is the resistance to fracture. Itshows the toughness of a material and also it shows how much fracture is created in the material. It can be calculated using the equation

$$Kc = \frac{P}{\beta C^{\frac{3}{2}}}$$

Where β is the indenter constant equal to 7 for Vickers indenter and C is the crack length measured from the center of the indentation mark on the sample. The calculated values of fracture toughness at 50 g are

6.728×10^5kg $m^{-3/2}$and 7.021×10^5kg $m^{-3/2}$ respectively for undoped and magnesium sulfate-doped L-leucinium oxalate crystals.

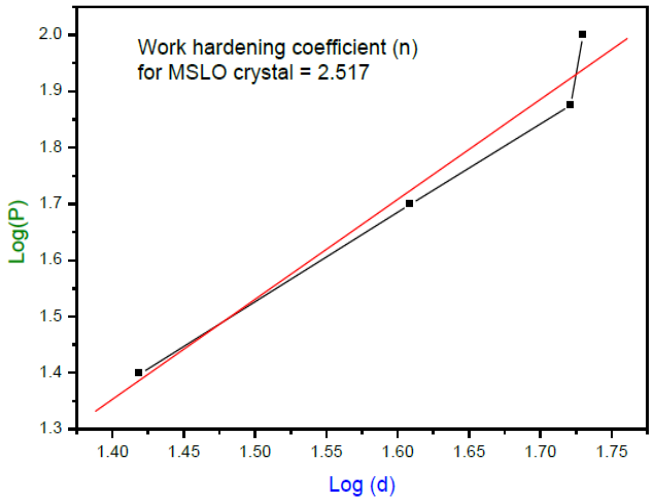

Fig. 18: Plot between log (d) and log (P) for MSLO crystal

3.4.3. Brittleness

Brittleness is an important parameter which disturbs the mechanical behavior of a material. Value of brittleness index (B_i) can be found using the equation

$$B_i = H_v / K_c$$

Estimated values of brittleness index at 50 g are 7.16×10^{-5} and 8.05×10^{-5} respectively for undoped and magnesium sulfate-doped L-leucinium oxalate crystals.

Since, the values of hardness, fracture toughness and brittleness index of MSLO crystal are large, the grown crystal shall be useful in fabrication of NLO devices. Values of hardness, yield strength and stiffness constant are given in table 2.

3.5. SHG efficiency

Kurtz and the Perry powder technique [25] was adopted to determine the relative Second Harmonic Generation (SHG) efficiency of MSLO crystalline sample. Beam of Nd: YAG laser was focused on the powdered sample of the crystal. Wavelength 1064 nm, pulse width 8ns and repetition rate of 10 Hz was used. Emission of green radiation at 532 nm indicates the SHG property and the values in connection with this test are provided in the table 3. KDP is used as reference sample. It emits green laser radiation of output energy of8.8 mJ/pulse. For comparison purpose, the SHG study was also carried out for undoped L-leucinium oxalate crystal. It emitted the green laser radiation of output energy of 7.81 mJ/pulse. The grown MSLO crystal emits the green laser radiation of output energy of 10.05 mJ/pulse and hence the relative SHG efficiency of MSLO crystal is 1.14 times that of KDP crystal. Since magnesium sulfate-doped L-leucinium oxalate (MSLO) crystal has more SHG efficiency than thatundoped L-leucinium oxalate and potassium dihydrogen phosphate (KDP) crystals, the grown crystal of MSLO could be used for better NLO applications.

Table 2: Hardness, yield strength and stiffness constant for MSLO crystal

Applied Load (g)	Hardness (kg/mm^2)	Yield strength 10^6 (pascal)	Stiffness constant (pascal)
10	55.10	2.422459	1.91276E+15
20	101.9	4.480010	5.60984E+15
30	137.0	6.023174	9.41687E+15
50	195.3	8.586320	17.5136E+15
70	220.6	9.698629	21.6748E+15
80	205.4	9.030364	19.1292E+15
100	187.2	8.230205	16.2623E+15

Table 3: SHG data obtained from Kurtz-Perry technique

Sl. No.	Sample Code / Name of the sample	Output Energy (milli joule/pulse)	Input Energy (joule/pulse)
1	KDP (Reference)	8.80	0.70
2.	Undoped L-leucinium oxalate	7.81	0.70
2	MSLO crystal	10.05	0.70

3.6. Laser damage threshold study

Laser damage threshold (LDT) damage in NLO crystals is usually caused by avalanche and multi-photon ionizations and temperature rise in the sample etc. and it depends on many factors like wavelength, energy, pulse duration, longitudinal and transverse modes and beam size [26]. Laser damage threshold (LDT) value of grown crystal was measured using an Nd: YAG laser of

wavelength of 1064 nm and pulse width of 10 ns. The laser beam with 1 mm diameter was focused by 30 cm focal length lens. To vary the energy of laser pulses an attenuator was employed. Pulse energy of every shot was determined by combining an oscilloscope and a phototube. "The value of LDT was estimated using the formula $\frac{E}{\pi\tau r^2}$ where E is the input energy in mJ/pulse, τ is the pulse width and r is the radius of the laser spot. The calculated value of LDT of MSLO crystal is 1.85 GW/cm^2. Since LDT value of this crystal is observed to be quite a large value and hence the grown crystal of MSLO could be used as the better crystal in NLO and laser applications.

3.7. Energy Dispersive Spectral (EDS) Analysis

Precise identification of the components in a crystal is an essential requirement for microanalysis. EDAX-INCA Instrument is applied to confirm the composite elements of the grown crystal. The recorded EDS spectrum of MSLO crystal is shown in fig.19. From the figure, we can see that, the MSLO crystal hasvarious elements such as Mg, S and C, N, O.

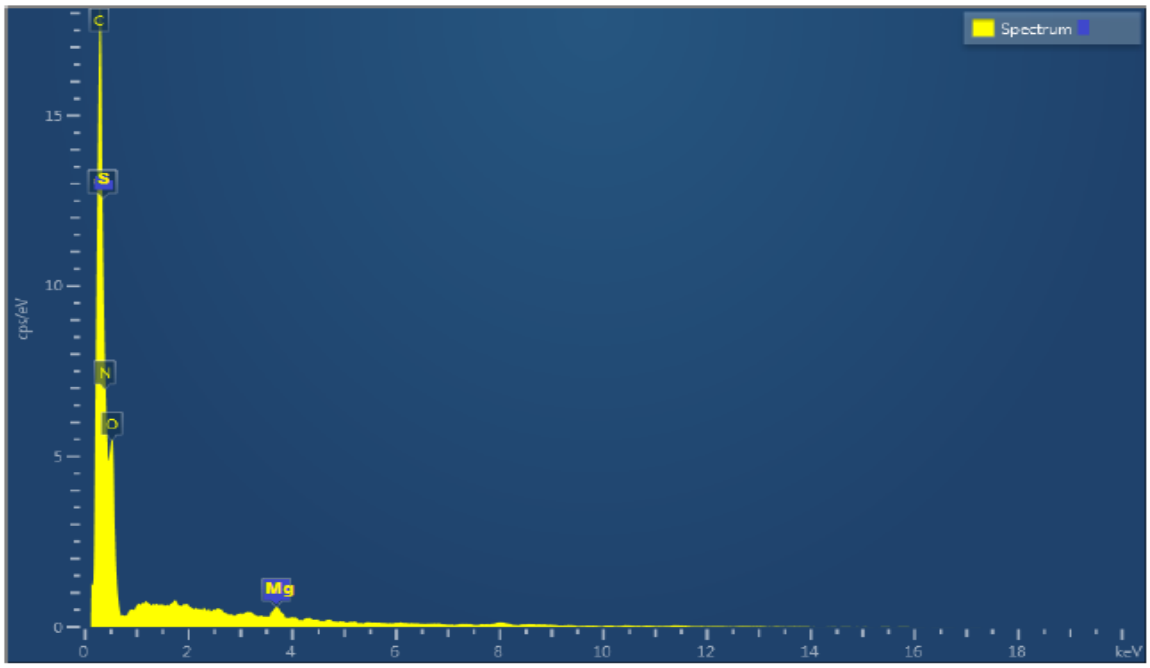

Fig. 19: EDS spectrum of MSLO crystal

4. CONCLUSION

Magnesium sulfate-doped L-leucinium oxalate (MSLO) single crystals were grown by slow evaporation technique at room temperature (30°C). Structural analysis was carried out by single-crystal X-ray diffraction study and the lattice parameters of MSLO crystal were determined. The data reveals that, MSLO crystal crystallizes in triclinic structure with space group P1. The optical transmittance study was done to find various linear optical parameters such as band gap, reflectance, refractive index, absorption coefficient, extinction coefficient, optical conductivity. The spectrum reveals that the grown MSLO crystal's lower cut-off wavelength is 218 nm. The calculated value of band gap is 5.69 eV and this value is observed to be high. The extinction coefficient increases slightly with increase of wavelength. The reflectance of the sample is low. The refractive index is observed to be increasing with increase of photon energy. Impedance studies were performed for the grown sample to understand the electrical properties. It is found that, as the frequency increases, both the real and imaginary components of impedance decreases and appears to converge at the higher frequency side. Further, as the temperature increases, the impedance values increase and this indicates that the sample has the negative temperature coefficient. Vickers Microhardness study was carried out to find the mechanical properties such as hardness, work hardening coefficient, brittleness index and fracture toughness of the grown MSLO crystal. It is seen

that the values of average diagonal indentation length (d) are increasing as the applied load increases and value of d of MSLO crystal is observed to be less compared to that of undoped L-leucinium oxalate crystal. Hardness is observed to be more for MSLO crystal. Work hardening coefficient is found to be 2.236. Kurtz-Perry powder technique with Nd: YAG laser was employed to study the second harmonic generation (SHG) efficiency. SHG efficiency of MSLO crystal is 1.14 times that of KDP crystal. Z-scan technique was used to fine the third-order NLO parameter of the sample. The nonlinear third-order optical susceptibility of MSLO crystal is higher than those of many other crystalline materials. The result indicates that the wavelength of the emitted light is greater than excitation wavelength. LDT study was also done for MSLO crystal. The calculated value of LDT of MSLO crystal is 1.85 GW/cm^2. Since LDT value of this crystal is observed to be quite a large value, the grown crystal of MSLO could be used as the better crystal in Laser applications. SEM and EDS studies were conducted on MSLO crystal to identify elements present in the sample. From EDS Spectrum, it is noted that, the grown MSLO crystal contains the elements like Mg, S and C, N, O.

5. ACKNOWLEDGMENTS

The authors are grateful to the staff members of various research centres such as the SAIF- IIT, Madras, ACIC - St. Joseph's College, Trichy, Cochin University, Cochin and VIT (Vellore) for their support in providing the research outputs.

Conflicts of Interest

The authors declare no conflict of interest.

Source of Funding

This research did not receive any specific grant from funding agencies in the public, commercial or non-profit sectors.

6. REFERENCES

1. Reena I, Arunkumar A. *Journal of Crystal Growth,* 2017; **457**:104-106.
2. Bhat SG, Dharamaprakash SM. *Journal of Crystal Growth*, 1997; **81**: 390-394
3. Jayaprakash M, Peer Mohamed P, Krishnan M, Nageshwari G, Lydia Caroline. *Physica B: Condensed Matter,*2016;**503**:25-31
4. Rajan Babu HD, EzhilVizhi R, Bhagavannarayana G. *Journal of Crystal Growth,* 2015; **423**:22-27.
5. KathiravanV, Satheesh Kumar G, Pari S, Selvarajan P. *Journal of Molecular Structure,* 2021;**1223**:128958.
6. Jeeva S, Muthu S, Tamilselvan M, Lydia Caroline P, Purushothaman S, Sevvanthi G, Vinitha G. *Chinese Journal of Physics,* 2018; **56**: 1449-1466.
7. Sonia,Vijayan, MahakVij, Harsh Yadav, Ravinder Kumar, Debashish Sur, Budhendra Singh. *Journal of Physics and Chemistry of Solids,* 2019; **129**:401-412.
8. Ramesh Babu R, Vijayan N, Gopalakrishna R, Ramasamy P. *Cryst. Res.Tech.,* 2006; **41**:405-410.
9. Saravanan N, Santhanakrishnan S, Suresh S. *J Mater Sci: Mater Electron*, 2018; **29**:18449-18457.
10. Sivakumar V, Jaisankar G, Chakkaravarthi G, Anbalagan, *Materials Letters*, 2014; **132**:298-301.
11. Anbuchezhiyan, Ponnusamy, Muthamizhchelvan. *Optoelectronics and Advanced Materials-Rapid Communications*, 2009; **3**:1161-1167.
12. Baskaran, Rajasekar S, Kumar M, Vimalan M, Selvaraju K. *Archives of Applied Science Research,* 2014; **6**:90-98.
13. Yadav S, Kumari M, Nayak D. *J. Electron. Mater.* 2020; **49:**7502-7508.
14. Rajagopal R, Krishnakumar V, SubhaNandhini R, MalathS, Rajan S, Natarajan S. *Acta Crystallo-graphica Section Structure Reports*, 2003; **E59**:878-880.
15. Raja, Seshadri S, Saravanan. *Optik*, 2014; **125**:916-919.
16. Sivavishnu, Srineevasan R, Johnson J. *Materials Science for Energy Technologies*, 2018; **1**: 205-214.
17. Bhuvana, Periyasamy K, Robinson, Jebas S, Gopala-krishnan N, Balasubramanian T. *Materials Letters*, 2007; **61**:4246-4249.
18. Shanthi A, Selvarajan P, Perumal S. *Optik*,2016; **127**:3192-3199.
19. Aly K. *J Mater Sci: Mater Electron,* 2022; **33**:2889-2898.
20. Gaffar, Abu El-Fadl A, Bin Anooz S. *Physica B: Condensed Matter,* 2003; **327**:43-54.
21. Surekha, Gunaseelan R, Sagayaraj P, Ambujam K. *The Roy. Soc. Chem.,* 2014; **16:**7979-7989.
22. Balakrishnan, Ramamurthi K. *Mater. Lett.*, 2008; **62:**65-68.
23. Abu El-Fad, Soltan JAS, Shaala NM. *Cryst. Res. Technol*, 2007; **42**:364-377.
24. Shanthi A, Selvarajan P, Jothi Mani R. *Optik*.2014; **125**:2531-2537.
25. Kurtz, Perry. *J. Appl.Phys.* 1968; 39:3798.
26. Karuppasamy K, Muthu Senthil Pandian, Ramasamy P, Sunil V. *Optical Materials,* 2018; **79:**152-171.